

Quantification of scattering changes using polarization-sensitive optical coherence tomography

Sang-Won Lee
Jin-Ho Kang
Ji-Yeong Yoo
Moon-Sik Kang

Yonsei University
Department of Biomedical Engineering
Wonju, South Korea

Jung-Tack Oh

Samsung Electronics Company, Limited
Suwon, Gyeonggi, Korea

Beop-Min Kim

Yonsei University
Department of Biomedical Engineering
234, Maeji, Heungup
Wonju, Kangwon-Do, South Korea

Abstract. We demonstrate that changes in the degree of polarization (DOP) depend on changes in the scattering coefficient, and they can be quantified by using a polarization-sensitive optical coherence tomography (PS-OCT) system. We test our hypothesis using liquid and solid phantoms made from Intralipid suspensions and gelatin, respectively. We also quantify the DOP changes with depth caused by changes in the concentration of scatterers in the liquid and solid phantoms. It is clearly shown that the DOP change has a linear relationship with the scattering change. In our previous study, we showed that the axial slope of the DOP is different between normal and pathologic cervical tissues. Our results demonstrate that the quantification of the axial DOP slope can be used for the systematic diagnosis of certain tissue pathology. © 2008 Society of Photo-Optical Instrumentation Engineers. [DOI: 10.1117/1.2976430]

Keywords: Polarization-sensitive optical coherence tomography; scattering property changes quantification; polarization degree.

Paper 08009RR received Jan. 9, 2008; revised manuscript received May 6, 2008; accepted for publication May 29, 2008; published online Sep. 5, 2008.

1 Introduction

The noninvasive and accurate measurement of linear optical properties such as absorption and scattering coefficients in biological tissues is essential for medical diagnosis.¹⁻⁷ It is also well known that for biological tissues under certain pathologic conditions such as dysplasia or carcinoma, scattering changes can occur due to variations in the refractive index mismatch between the intracellular fluid (or cellular components) and extracellular fluid.^{1,2} Additionally, the sizes of cellular nuclei may be increased and the structural protein density may be decreased, which can contribute to the tissue scattering changes.³ Therefore, the measurement of the change in the scattering coefficient may facilitate the discrimination between normal and abnormal tissues.^{2,3}

Elastic-scattering spectroscopy, diffuse optical tomography, confocal microscopy, and optical coherence tomography (OCT) have been studied as optical diagnosis tools that measure the scattering change or scattering coefficient.¹⁻⁷ Elastic-scattering spectroscopy and diffuse optical tomography have been used to diagnose prostate cancer, breast cancer, and morphological changes in epithelial tissues such as those in the skin, gastrointestinal tract, and cervix.⁴⁻⁶ These techniques, which are sensitive to both scattering and absorption properties, can discriminate morphological changes in tissues and detect backscattered light from deep within biological tissues. In confocal microscopy, the exponential attenuation of the light intensity along the axial direction can be described by the Beer-Lambert law, $I=I_0 \exp(-\mu_t z)$, where z denotes the axial path and μ_t denotes the total attenuation coefficient,

which is the sum of the absorption coefficient (μ_a) and the scattering coefficient (μ_s). Since for many tissues ($\mu_a \ll \mu_s$ in the near-infrared spectral range), scattering changes can be detected by obtaining the exponential slope of the light attenuation with depth.³ Confocal microscopy has been used for estimating the scattering coefficient from regions of a normal and precancerous cervical epithelium.³ The results suggest that a large scattering due to high-density cell nuclei in high-grade dysplasia can be observed in the entire epithelium under pathologic conditions.

Recently, several research groups have proposed and studied OCT as a measurement tool for scattering changes.^{1-3,7} OCT is an imaging technique that provides a high-resolution cross sectional image of biological tissues. Using OCT, the scattering changes can be detected by means of obtaining the exponential slope of the light attenuation with depth, in a manner similar to confocal microscopy.^{1-3,7} The OCT system has also been studied for noninvasive glucose monitoring. An increase in the glucose concentration in a turbid medium or biological tissue reduces the refractive index mismatch and thus reduces the scattering coefficient.² A similar methodology has been employed for the diagnosis of cervical cancer by measuring the slope of the intensity signal decay with depth.⁷ The results show that the slope of the intensity decay in normal tissue is lower than that in abnormal tissue. However, this method has a limitation, in that the decay slope can be significantly affected by the location of the focal point. A nonflat tissue surface and motion artifacts can lead to the misinterpretation of the intensity decay slope.²

It is well known that the scattering also affects the polarization state during the propagation of polarized light in turbid media. Polarized light incident to a highly scattering medium

Address all correspondence to Beop-Min Kim, Department of Biomedical Engineering, 234, Maeji, Heungup, Wonju, Gangwon-Do, South Korea; Tel: +82-33-760-2490; Fax: +82-33-766-2464; E-mail: <mailto:beopkim@yonsei.ac.kr> beopkim@yonsei.ac.kr.

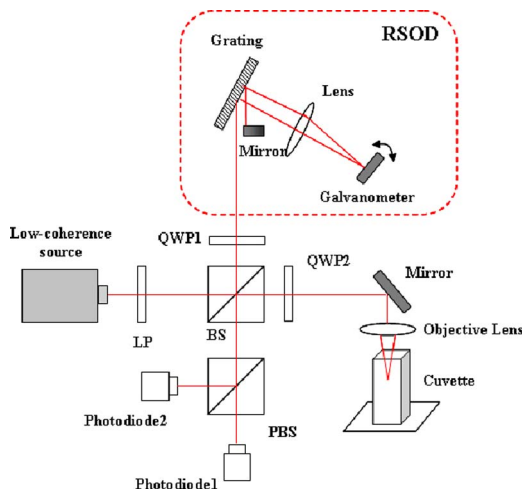


Fig. 1 Schematic diagram of the PS-OCT system with a rapid scanning optical delay line (RSOD). LP: linear polarizer. BS: beamsplitter. QWP: quarter-wave plate. PBS: polarization beamsplitter.

is multiply scattered and depolarized.^{8–11} The depolarization can be attributed to the size and shape of the scatterer, the initial polarization state (circular or linear) of the light incident to the medium, and the optical properties of the medium. When the incident light is linearly polarized, the degree of polarization (DOP) from the backscattered light decays exponentially.⁸ Further, if circularly polarized light is incident on a scattering medium, the depolarization effect is different.^{9–11} When the incident light is circularly polarized in forward-scattering media (a large anisotropy factor, i.e., large-sized particles), the single-scattered light returned is circularly polarized and has the opposite helicity. Therefore, the DOP decays to near zero initially (or at shorter path lengths); it then increases again and tends to decay down to zero (depolarization).^{9,10} However, if the incident light is circularly polarized in scattering media comprising small-sized particles, the DOP is not affected by the helicity.^{9,11} Previous studies have simulated and measured these phenomena according to changes in the particle size or concentration, even if the depolarization has not been quantified.^{8–11}

In this work, we demonstrate a polarization-sensitive OCT (PS-OCT) system that can provide not only cross-sectional images, but also information regarding the polarization state of the light reflected back from the turbid media to measure and quantify the depolarization caused by scattering in Intralipid suspensions. The depolarization can be quantified by estimating the DOP changes with depth.

2 Materials and Methods

We assume two hypotheses in this study: 1. since the DOP change with depth can be normalized by the reflected light intensity, the location of the focal point does not affect our readings; and 2. the DOP change with depth is affected by the scattering properties. To verify these hypotheses, we constructed a typical PS-OCT system, as shown in Fig. 1.^{12,13} A superluminescence diode (SLD) with a center wavelength of 1300 nm and a bandwidth of 40 nm was used as the light source. Light in the reference arm passes through a quarter-wave plate (QWP) oriented at 22.5 deg with respect to the

horizontal axis, so that the reflected light has a 45 deg linear polarization state after the roundtrip. A QWP in the sample arm, oriented at 45 deg with respect to the horizontal axis, provided circularly polarized light to the sample. The detected signal was digitized by an analog-to-digital converter and filtered using a digital bandpass filter. We obtained the amplitudes and phases by using the Hilbert transformation. To determine the polarization state of the light in the medium, the Stokes parameters were computed as follows^{12,13}:

$$S_0 = A_H^2 + A_V^2,$$

$$S_1 = A_H^2 - A_V^2,$$

$$S_2 = 2A_H A_V \cos(\Delta\alpha),$$

$$S_3 = 2A_H A_V \sin(\Delta\alpha), \quad \Delta\alpha = \alpha_H - \alpha_V, \quad (1)$$

where A_H and A_V denote the amplitudes, and α_H and α_V denote the phases in the horizontal and vertical channels, respectively. Because the light reflected from the sample had to pass through the QWP (oriented at 45 deg) in the sample arm for a second time, the Stokes parameters S_1 and S_3 would be exchanged.¹³ Additionally, the DOP was calculated as¹³

$$\text{DOP} = (S_1^2 + S_2^2 + S_3^2)^{1/2} / S_0.$$

For axial scanning, we used a rapid-scanning optical delay line (RSOD) method with a scan rate of 200 Hz corresponding to a Doppler (carrier) frequency of 65 kHz and 5000 sampling points per single A-line.^{14,15} The axial depth scan range was approximately 2 mm.

In this study, we used the DOP profile with depth to quantify the scattering properties for both liquid and solid phantoms that contain 2.5, 5, and 10% Intralipid suspensions as scatterers. Each sample was scanned over a surface in a manner similar to conventional 2-D OCT imaging, and the signals were averaged over 1000 A-lines.

In our previous study, to demonstrate that our method is applicable to clinical diagnosis, we quantified the scattering changes of normal and malignant cervical tissues.¹⁶ A part of these results is duplicated in this work.

3 Results

3.1 Optical Phantoms

The circularly polarized light is incident on the top surface of the sample, which is contained in a cuvette, as shown in Fig. 2(a). The DOP of each A-line is always unity (DOP=1), because conventional PS-OCT systems are amplitude-based detection systems employing heterodyne receivers that detect the electric field of only the coherent part of the backscattered light.¹⁷ However, if the DOP is calculated after averaging the Stokes parameters for all the A-lines (spatially), the DOP decreases because the scattering effect is similar to random processing. Figure 2(b) shows the DOP signal as a function of the depth in a 10% Intralipid suspension measured using the PS-OCT system. Because the mean particle size in the Intralipid suspension (approximately 200 to 300 nm, $g \approx 0.35$ at 1300 nm)¹⁸ used in this study is smaller than the wavelength

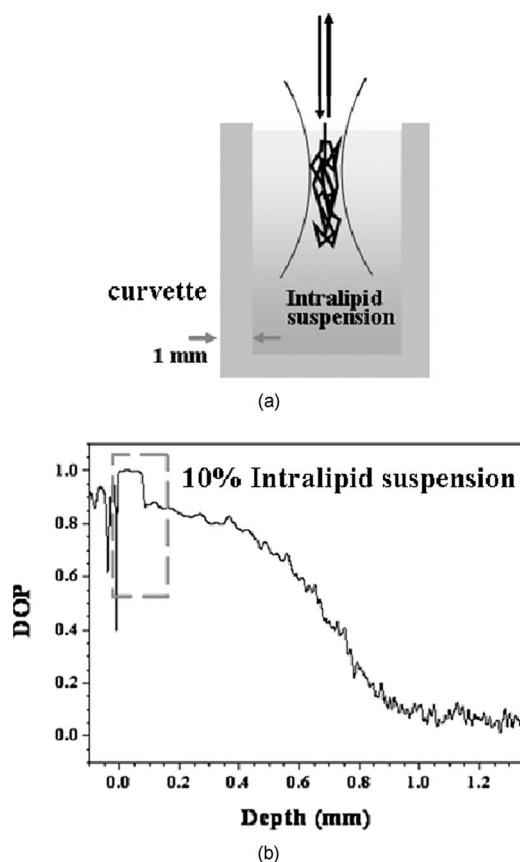


Fig. 2 (a) Phantom solution contained in a cuvette. The incident light is circularly polarized and the backscattered light from the sample is detected by the PS-OCT system. (b) Measured profile of the DOP signal in 10% Intralipid suspension.

of our light source (1300 nm), it is isotropic scattering that is largely responsible for the depolarization of the light. Therefore, although the scattering coefficient of the Intralipid suspension is large, the DOP signal does not significantly exhibit the effect of helicity [see square box in Fig. 2(b)]. If the effect of helicity is significant, the DOP decays to near zero initially (or for shorter path lengths), then increases again and decays down to zero due to depolarization, as reported in other studies.^{9,10}

The DOP change is induced by several effects, including depolarization by scattering, phase retardation by birefringence, and noise fluctuation artifacts. In our experiments, we excluded the effects of birefringence, because the Intralipid suspensions are isotropic scattering media. To demonstrate that the DOP is strongly affected by not only the noise but also the scattering changes, we compared the back-reflected intensity signal with the DOP signal in 2.5 and 10% Intralipid suspensions, and a mirror with a variable neutral density (ND) filter. In Fig. 3, the DOP profile is drawn against the intensity signal level signal-to-noise ratio (SNR). When no scattering exists, as in the case of the mirror with a variable ND filter placed in the sample arm (upper graph in Fig. 3), it is shown that the DOP is maintained until the SNR reaches down to approximately 30 dB. When the signal level drops below 30 dB, the DOP begins to decrease due to electrical noise. When scattering exists (2.5 and 10% Intralipid suspensions),

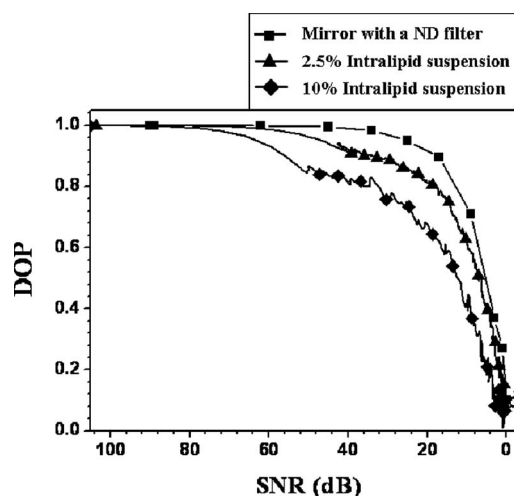


Fig. 3 The back-reflected intensity signal level (SNR) versus the degree of polarization (DOP). The figure shows that the DOP is strongly affected by an increase in the scattering in addition to the noise.

the DOP begins to decrease at a higher SNR level above 30 dB. Further, it is clearly shown that when the scattering coefficient increases, the DOP began to decrease at even higher SNR values. These data demonstrate that the depolarization changes are affected not only by the noise but also by the scattering changes.

We used the DOP profile with depth to quantify the scattering properties for both the Intralipid solution and solid gelatin phantoms with scatterers. Each sample was scanned and the signals were averaged over 1000 A-lines. It appeared that the profile comprised a single-scattering region (shallow) and a multiple-scattering region (deep). We fitted the DOP profile with a sigmoid shape using various mathematical models, and found that a simple Boltzmann equation was more useful than typical polynomials. The simple Boltzmann equation is expressed as follows:

$$y = A_2 + (A_1 - A_2) \left/ \left[1 + \exp\left(\frac{x - x_0}{dx}\right) \right] \right., \quad (2)$$

where A_1 and A_2 denote the initial y value (when $x = -\infty$) and final y value (when $x = \infty$), respectively. The approximate range of dramatically change is dx , and x_0 denotes the center of the range. An example of the data and our fitting results is shown in Fig. 4. One of the fitted parameters, x_0 , discriminates the single-scattering and multiple-scattering regions. We found that this parameter is sensitive to the scattering changes.

We used 2.5, 5, and 10% Intralipid suspensions and solid phantoms made of gelatin for the DOP measurements. Again, each sample was scanned and averaged over 1000 A-lines, a procedure that was repeated at five different locations per sample. The transverse B-scanning was done only for the solid phantoms, since the random Brownian motion of the liquid naturally reduces the speckle noise. The DOP signals were quantified based on the methodology presented earlier. Figures 5(a) and 5(b) show the results obtained from the liquid phantoms and the solid phantom, respectively. As expected, as the scattering coefficient increases, the DOP decays

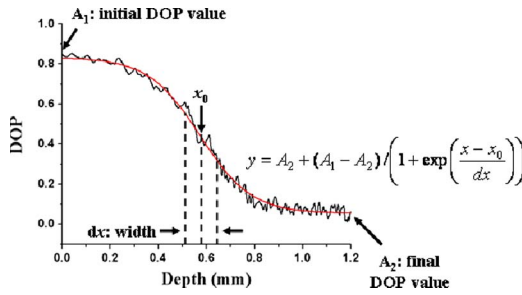


Fig. 4 Fitted results of the DOP signal using a simple Boltzmann equation. A_1 : initial DOP value. A_2 : final DOP value. x_0 : center depth of the region where the DOP drastically changes. dx : width.

faster and the location of the x_0 parameter moves toward the surface. Further, it is clearly observed that the DOP changes linearly ($R \approx 0.99$) with the scattering changes for both sets of phantoms. It has been reported that, in liquid phantoms, the DOP decays due to the Brownian movement of the particles when PS-OCT is used for DOP measurements.¹⁷ However, in Fig. 5(b), it is clearly observed that the DOP change has linear relationships ($R \approx 0.99$) for solid phantoms, as found in the liquid phantom studies. Our results imply that it is possible to measure the scattering changes without the effect of Brownian movement, and moreover, PS-OCT is effective for this pur-

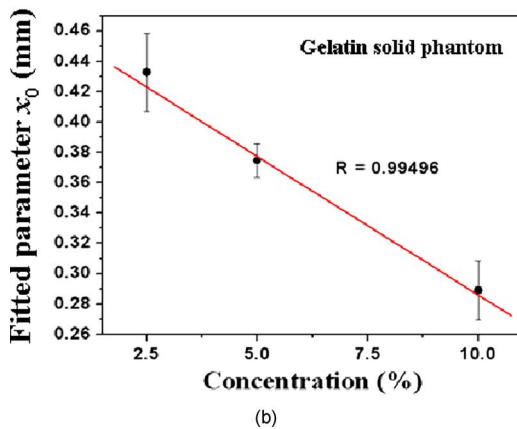
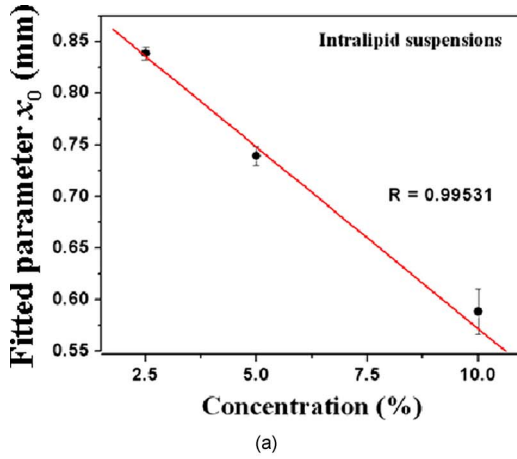


Fig. 5 PS-OCT results for scattering measurements. Linear relationships are evident for both (a) liquid phantom and (b) solid phantom.

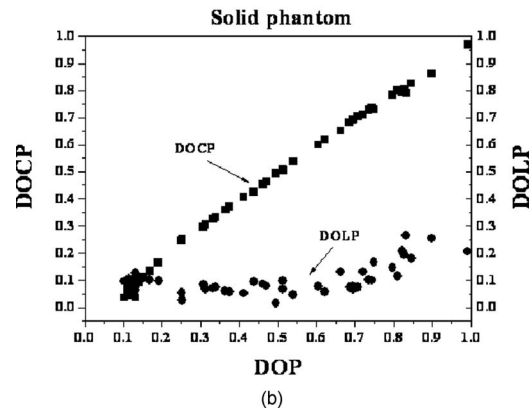
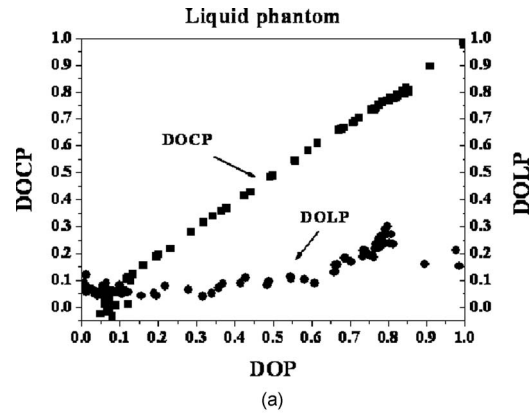


Fig. 6 The degree of circular polarization (DOCP) and the degree of linear polarization (DOLP) profiles drawn against the DOP. The DOCP changes contributed significantly to the DOP changes when circularly polarized light was incident onto the scattering medium of (a) liquid and (b) solid states without phase retardation due to birefringence.

pose. Although the Intralipid concentration in the solid phantoms was the same as that in the liquid phantoms, the fitted results were differently described because of the refractive index mismatch between gelatin and water. Also, the difference in Brownian motion between solid and liquid phantoms prevents direct comparison of the fitted parameters.

Figures 6(a) and 6(b) show the degree of circular polarization (DOCP) and the degree of linear polarization (DOLP) profiles in liquid and solid phantoms, which are calculated as

$$\text{DOCP} = \sqrt{S_3^2}/S_0 \text{ and } \text{DOLP} = \sqrt{S_1^2 + S_2^2}/S_0,$$

respectively,^{13,17} drawn against the DOP. These results demonstrate that the DOCP is similar and linearly proportional to the DOP when circularly polarized light is incident onto the scattering medium, assuming no phase retardation due to birefringence.

To verify our first hypothesis, we measured the effects of the location changes of the focused beam by using 2.5% Intralipid suspensions. In the sample arm, the diameter of the collimated beam was approximately 2 mm. We used an objective lens (10 \times , NA=0.25) with a focal length of 18 mm. Therefore, a depth of view and transversal resolution were 120 and 13 μm , respectively. The back-reflected intensity signal was also exponentially fitted using the Beer-Lambert law,

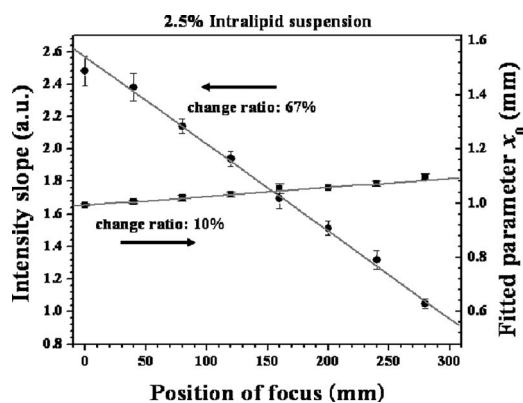


Fig. 7 Effects of the position of the focal point. The scattering measurements using the back-reflected intensity signal are considerably more sensitive to the location of the focal point at which they were measured by the PS-OCT system.

and the results are compared in Fig. 7. The focal location varied from the surface to a depth of $280\ \mu\text{m}$ in steps of $40\ \mu\text{m}$. As shown in Fig. 7, the intensity profile is greatly affected by the focal position (67% change). When the DOP was used, the change was only 10%, which shows that PS-OCT may be a superior tool for scattering measurements.

3.2 Biological Samples

Cervical intraepithelial neoplasia (CIN) is a precancerous condition of the cervix. It induces morphological changes in the cervical epithelium, which increases the nuclear/cytoplasmic (N/C) area ratio.³ Since the nucleus is one of the significant scatterers in the cervix, the increase in the N/C area ratio induces an increase in the scattering coefficient³ and affects the light depolarization process.

In our previous study, we measured the axial slope of the DOCP decay in the epithelial region for both normal and abnormal [CIN-III, and cervical intraepithelial carcinoma (CIS)] cervical tissues.¹⁶ 25 cervical areas were examined from five cone-biopsy samples. 16 areas were found to be normal, while others were abnormal. Immediately after the cone biopsy, each sample was imaged using the PS-OCT system. The samples were then stained with hematoxylin and eosin (H and E) and read by a physiologist. We excluded the effects of birefringence, since it is known that there are no collagen fibers in the epithelium of the cervix except at the basement membrane, which comprises type 4 collagen.^{3,19} Since there exists no phase retardation due to collagen inside the cervical epithelium, the DOCP is almost the same as the DOP, as shown in Fig. 6, which is why we used the DOCP to simplify the calculation. The epithelium is not sufficiently thick for the full Boltzmann fitting to be applied. Therefore, we simply performed a linear fitting for the DOCP data obtained from depths of 80 to $300\ \mu\text{m}$. Since the tissue surface was not flat, the surface location for each A-scan signal was first determined, and the DOCP data were averaged over the entire area. Figure 8, reproduced from Ref. 16, shows that the averaged axial slopes of the DOCP decay were 0.92 and $1.71\ \text{mm}^{-1}$ in normal and abnormal cervix tissues, respectively ($p < 0.01$). The error bars in the graph represent the standard deviations for each dataset. The unit of the fitted parameters in the

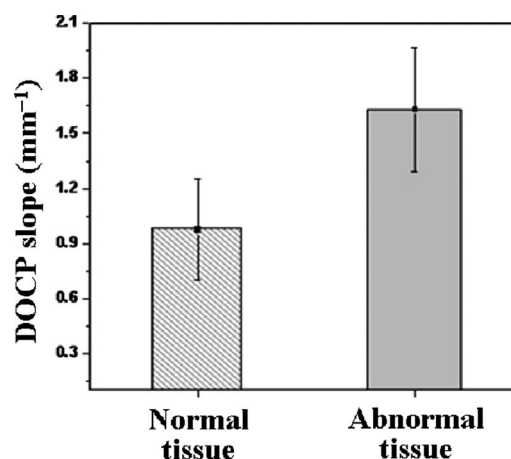


Fig. 8 The averaged slopes of the DOCP between normal and abnormal cervical tissues. As expected, the DOCP decays faster for abnormal conditions due to the higher scattering. Reproduced from Ref. 16.

sample tissues was different from that in the phantoms, because different fitting algorithms were applied. However, it is evident that the DOCP decays faster for abnormal tissues because of the scattering increase, which is consistent with the phantom data.

4 Discussion

In this study, we used the PS-OCT system to quantify the DOP changes caused by the scattering changes in liquid phantoms, solid phantoms, and biological samples. Other groups have studied the depolarization pattern depending on changes in the particle size or concentration using an OCT or a PS-OCT system.^{17,20} Schmitt and Xiang²⁰ measured and quantified the depolarization using a conventional OCT system before the first PS-OCT system for biological sample imaging was introduced by de Bore, Milner, and Nelson.²¹ They used a linear polarizer to polarize the incident beam. Then, by manually rotating a QWP on the reference arm, they collected the copolarized and cross-polarized lights to measure two of the four Stokes parameters. In addition, they arbitrarily defined the depolarization ratio as the ratio between copolarization and cross-polarization interference intensities, which is different from the conventional definition of the DOP. They showed that the depolarization ratio increased with the particle size or scatterer concentration, which is consistent with our results.

Jiao, Yao, and Wang also performed similar measurements using a PS-OCT system.¹⁷ They delivered four different polarizations (horizontal, vertical, right circular, and left circular) in both the sample and reference arms and found 4×4 Mueller matrix images. In their phantom studies, the DOP, DOLP, and DOCP were calculated by having only horizontally polarized light incident on the sample and changing the polarization of the beam on the reference arm. They showed that the DOP could be changed for Intralipid concentrations of 1, 2, and 5%, and proposed that the DOP changes were caused by the Brownian motion of the particles in the liquid.¹⁷ In addition, the authors reported that all the DOP data were unity at all depths scanned over solid fish bone.¹⁷ This is theoretically correct since OCT is a coherence gating technique. One of the major differences between the study in Ref. 17 and ours

is that we collected each A-scan datum, averaged the raw data (Stokes parameters) first, and then calculated the DOP both for liquid and solid phantoms. In this manner, we can expect the “polarization scrambling effect,” which results in subunity DOP values for both liquid and solid samples. As shown in Fig. 3, we demonstrated that the DOP decrease is not only caused by the noise but also by actual scattering changes that can be quantified.

Our method is applicable to homogeneous media such as the phantoms we used. To show that this methodology is also applicable to clinical diagnosis, we presented the results of our previous studies (Fig. 8). The detection of intraepithelial neoplasia in the cervix or lung can be a target application, assuming that the epithelial tissues are homogeneous. Our preliminary study shows that our technology can potentially be applied for clinical studies; however, more clinical studies are required.¹⁶

We showed that our technology is insensitive to the location of the focal point, which is very important in clinical settings. Conventional OCT technology can be used for the quantification of scattering changes, assuming that the position of the focal point is maintained at a certain depth throughout the B-scans, which is difficult to control, since the tissue surfaces are usually not flat. Using our technology, the scattering changes can be estimated more reliably.

5 Conclusion

In conclusion, we demonstrate that changes in the scattering coefficient can be quantified by using the PS-OCT system. In liquid and solid phantoms, the axial DOP profile is fitted to a Boltzmann equation and the parameter is found to be linearly dependent on the scattering changes. It is also shown that the scattering measurements using PS-OCT are much less sensitive to the location of the focal point, compared to the previously reported method that uses back-reflected intensity profiles. To demonstrate our hypothesis in biological samples, we quantify the axial DOCP decay profiles from normal and abnormal cervical tissues. The results show that the slope of the DOCP decay is largely affected by the pathology of the tissue, which involves the scattering property changes. Our studies indicate that the PS-OCT system may have potential to be used for the diagnosis of intraepithelial neoplasm.

Acknowledgments

This study was supported by a grant of the Korea Health 21 R&D Project, Ministry of Health & Welfare, Republic of Korea (02-PJ3-PG6-EV07-0002). This work was also supported by the Bio-signal Analysis Technology Innovation Program (M10645010001-06N4501-00110) of the Ministry of Science and Technology (MOST) and Korea Science and Engineering Foundation (KOSEF). This research was also supported by a grant (M103KV010023-08K2201-02310) from Brain Research Center of the 21st Century Frontier Research Program funded by the Ministry of Science and Technology, Republic of Korea.

References

1. A. I. Kholodnykh, I. Y. Petrova, M. Motamedi, and R. O. Esenaliev, “Accurate measurement of total attenuation coefficient of thin tissue

- with optical coherence tomography,” *IEEE J. Sel. Top. Quantum Electron.* **9**(2), 210–221 (2003).
2. R. O. Esenaliev, K. V. Larin, and I. V. Larina, “Noninvasive monitoring of glucose concentration with optical coherence tomography,” *Opt. Lett.* **26**(13), 992–994 (2001).
3. T. Collier, M. Follen, A. Malpica, and R. Richards-Kortum, “Sources of scattering in cervical tissue: Determination of the scattering coefficient by confocal microscopy,” *Appl. Opt.* **44**(11), 2072–2081 (2005).
4. J. R. Mourant, I. J. Bigio, J. Boyer, T. M. Johnson, J. Lacey, A. G. Bohorfoush, and M. Mellow, “Elastic scattering spectroscopy as a diagnostic tool for differentiating pathologies in the gastrointestinal tract: Preliminary testing,” *J. Biomed. Opt.* **1**(2), 192–199 (1996).
5. I. J. Bigio, S. G. Bown, G. Briggs, C. Kelley, S. Lakhani, D. Pickard, P. M. Ripley, I. G. Rose, and C. Saunders, “Diagnosis of breast cancer using elastic-scattering spectroscopy: preliminary clinical results,” *J. Biomed. Opt.* **5**(2), 221–228 (2000).
6. S. Fantini, S. A. Walker, M. A. Franceschini, M. Kaschke, P. M. Schlag, and K. T. Moesta, “Assessment of the size, position, and optical properties of breast tumors *in vivo* by noninvasive optical methods,” *Appl. Opt.* **37**(10), 1982–1989 (1998).
7. A. F. Zuluaga, M. Follen, I. Boiko, A. Malpica, and R. Richards-Kortum, “Optical coherence tomography: A pilot study of a new imaging technique for noninvasive examination of cervical tissue,” *Am. J. Obstet. Gynecol.* **193**(1), 83–88 (2005).
8. D. A. Zimnyakov, Y. P. Sinichkin, P. V. Zakharov, and D. N. Agafonov, “Residual polarization of non-coherently backscattered linearly polarized light: the influence of the anisotropy parameter of the scattering medium,” *Waves Random Media* **11**(4), 359–412 (2001).
9. I. Charalambous, R. Cucu, A. Dogariu, and A. Podoleanu, “Experimental investigation of circular light depolarization using polarization sensitive OCT,” *Proc. SPIE* **6429**, 64291S (2007).
10. M. Sakami, and A. Dogariu, “Polarized light-pulse transport through scattering media,” *J. Opt. Soc. Am. A* **23**(3), 664–670 (2006).
11. A. Ishimaru, S. Jaruwatanadilok, and Y. Kuga, “Polarized pulse waves in random discrete scatterers,” *Appl. Opt.* **40**(30), 5495–5502 (2001).
12. M. G. Ducros, J. F. de Boer, H. Huang, L. C. Chao, and Z. Chen, “Polarization sensitive optical coherence tomography of the rabbit eye,” *IEEE J. Sel. Top. Quantum Electron.* **5**(4), 1159–1167 (1999).
13. J. F. de Boer and T. E. Milner, “Review of polarization sensitive optical coherence tomography and Stokes vector determination,” *J. Biomed. Opt.* **7**(3), 359–371 (2002).
14. G. J. Tearney, B. E. Bouma, and J. G. Fujimoto, “High-speed phase- and group-delay scanning with a grating-based phase control delay line,” *Opt. Lett.* **22**(23), 1811–1813 (1997).
15. A. M. Rollins, M. D. Kulkarni, S. Yazdanfar, R. Ung-arunyawee, and J. A. Izatt, “*In vivo* video optical coherence tomography,” *Opt. Express* **3**, 219–229 (1998).
16. J. Y. Yoo, S. W. Lee, M. S. Kang, Y. T. Kim, and B. M. Kim, “Early-stage diagnosis of cervix using PS-OCT,” presented at the Photonics West 2006, Optical Biopsy VI, 6091–15, 21–26 Jan. 2006, San Jose, CA, SPIE.
17. S. Jiao, G. Yao, and L. V. Wang, “Depth-resolved two-dimensional Stokes vectors of backscattered light and Mueller matrices of biological tissue measured with optical coherence tomography,” *Appl. Opt.* **39**(34), 6318–6324 (2000).
18. H. J. van Staveren, C. J. M. Moes, J. Van Marle, S. A. Prahl, and M. J. C. Van Gemert, “Light scattering Intralipid-10% in the wavelength range of 400–1100 nm,” *Appl. Opt.* **30**(31), 4507–4514 (1991).
19. K. Carlson, I. Pavlova, T. Collier, M. Descour, M. Follen, and R. Richards-Kortum, “Confocal microscopy: Imaging cervical precancerous lesions,” *Gynecol. Oncol.* **99**(3), S84–S88 (2005).
20. J. M. Schmitt and S. H. Xiang, “Cross-polarized backscatter in optical coherence tomography of biological tissue,” *Opt. Lett.* **23**(13), 1060–1062 (1998).
21. J. F. de Boer, T. E. Milner, and J. S. Nelson, “Determination of the depth-resolved Stokes parameters of light backscattered from turbid media by use of polarization-sensitive optical coherence tomography,” *Opt. Lett.* **24**(5), 300–302 (1999).